Conductivity of Graphene with Resonant and Nonresonant Adsorbates

Guy Trambly de Laissardière[1] and Didier Mayou[2]

[1]*Laboratoire de Physique théorique et Modélisation, CNRS and Université de Cergy-Pontoise,*
95302 Cergy-Pontoise, France
[2]*Université Grenoble Alpes, Institut NEEL, F-38042 Grenoble, France,*
and CNRS, Institut NEEL, F-38042 Grenoble, France

We propose a unified description of transport in graphene with adsorbates that fully takes into account localization effects and loss of electronic coherence due to inelastic processes. We focus in particular on the role of the scattering properties of the adsorbates and analyze in detail cases with resonant or nonresonant scattering. For both models, we identify several regimes of conduction, depending on the value of the Fermi energy. Sufficiently far from the Dirac energy and at sufficiently small concentrations, the semiclassical theory can be a good approximation. Near the Dirac energy, we identify different quantum regimes, where the conductivity presents universal behaviors.

Electronic transport in graphene [1–4] is sensitive to static defects that are, for example, frozen ripples, screened charged impurities, or local defects like vacancies or adsorbates [5–8]. Adsorbates, which can be organic groups or adatoms attached to the surface of graphene, are of particular interest in the context of functionalization, which aims at controlling the electronic properties by attaching atoms or molecules to graphene [9–14]. Therefore, there is a need for a theory of conductivity in the presence of such defects.

Theoretical studies of transport in the presence of local defects have dealt mainly either with the Bloch-Boltzmann formalism or with self-consistent approximations [10,15–22]. In these theories, a major length scale that characterizes the electron scattering is the elastic mean-free path L_e. These approaches indeed explain some experimental observations such as the quasilinear variation of conductivity with a concentration of charge carriers [10–14]. Yet, these theories have important limitations and can hardly describe in detail the localization phenomena that have been reported in some experiments [6,7,11,12]. Indeed, in the presence of a short range potential, such as that produced by local defects, the electronic states are localized on a length scale ξ [23–26]. A sample will be insulating unless some source of scattering, like electron-electron or electron-phonon interaction, leads to a loss of the phase coherence on a length scale $L_i < \xi$. Therefore, in addition to the elastic mean-free path L_e, the inelastic mean-free path L_i and the localization length ξ also play a fundamental role for the conductivity of graphene with adsorbates.

In this Letter, we develop a numerical approach for the conductivity that treats exactly the tight-binding Hamiltonian and takes fully into account the effect of Anderson localization. This approach gives access to the characteristic lengths and to the conductivity as a function of the concentration, the Fermi energy E_F, and the inelastic mean-free path L_i. In real samples, L_i depends on the temperature, or magnetic field, but it is an adjustable parameter in this work. Our results confirm that sufficiently far from the Dirac energy and for sufficiently small adsorbate concentrations, the Bloch-Boltzmann theory and the self-consistent theories are valid when $L_e \ll L_i \ll \xi$. Near the Dirac energy, we identify different regimes of transport that depend on whether the adsorbates produce resonant or nonresonant scattering. These different regimes of transport present some universal characteristics, the consequences of which are discussed for experimental measurements of conductivity and magnetoconductivity.

Models of adsorbates.—The scattering properties of local defects like adsorbates or vacancies are characterized by their T matrix. Local defects tend to scatter electrons in an isotropic way for each valley and lead also to strong intervalley scattering. Yet, the energy dependence of the T matrix depends very much on the type of defect, and in this work, we focus on the role of this energy dependence. To this end, we consider two models for which the T matrix diverges at the Dirac energy (resonant adsorbates leading to midgap states also called zero-energy modes) or is constant (nonresonant adsorbates). Note that resonances can occur also at nonzero energy, but here we restrict ourselves to the important case of zero-energy modes. The conclusions drawn here, concerning the influence of the energy dependence of the T matrix for adsorbates, are useful for other types of local defects.

We consider that the adsorbates create a covalent bond with some atoms of the graphene sheet. Then, a generic model is obtained by removing the p_z orbitals of these carbon atoms [17–19,22–29]. For example, a hydrogen adsorbate can be modeled by removing the p_z orbital of the carbon atom that is just below the hydrogen atom. This is the model of resonant adsorbate that we consider here. In this case, the T matrix associated with the adsorbate

diverges at the Dirac energy, hence the name resonant scatterers. The nonresonant model is constituted by two neighboring missing orbitals (divacancy). In that case, the T matrix is nearly constant close to the Dirac energy and does not diverge.

Finally, we consider here that the up and down spins are degenerate; i.e., we deal with a paramagnetic state. Indeed, the existence of a magnetic state for various adsorbates, like hydrogen, for example, is still debated [30]. Let us emphasize that in the case of a magnetic state, the up and down spins give two different contributions to the conductivity but the individual contribution of each spin can be analyzed from the results discussed here. With these assumptions, the generic model Hamiltonian for adsorbates can be written as

$$H = -t \sum_{\langle i,j \rangle} (c_i^\dagger c_j + c_j^\dagger c_i), \quad (1)$$

where $\langle i, j \rangle$ represents nearest-neighbor pairs of occupied sites and $t = 2.7$ eV determines the energy scale. In our calculations, the vacant sites (resonant adsorbates) or the divacant sites (nonresonant adsorbates) are distributed at random with a finite concentration.

Evaluation of the conductivity.—The present study relies upon the Einstein relation between the conductivity and the quantum diffusion. We evaluate numerically the quantum diffusion using the Mayou-Khanna-Roche-Triozon approach [31–35]. This method has been used to study quantum transport in disordered graphene, chemically doped graphene, graphene with functionalization, and graphene with structural defects [13,14,26,29,36–41]. We introduce an inelastic scattering time τ_i, beyond which the propagation becomes diffusive due to the destruction of coherence by inelastic processes (relaxation time approximation) [42–47]. We finally get (see Sec. I of the Supplemental Material [48])

$$\sigma(E_F, \tau_i) = e^2 n(E_F) D(E_F, \tau_i), \quad (2)$$

$$D(E_F, \tau_i) = \frac{L_i^2(E_F, \tau_i)}{2\tau_i}, \quad (3)$$

where E_F is the Fermi energy, $n(E_F)$ the density of states (DOS), $D(E_F, \tau_i)$ the diffusivity, τ_i the inelastic scattering time, and $L_i(E_F, \tau_i)$ the inelastic mean-free path. $L_i(E_F, \tau_i)$ is the typical distance of propagation during the time interval τ_i for electrons at the energy E_F in the system without inelastic scattering [49].

The typical variation of $\sigma(\tau_i)$ in our study (see Sec. II of the Supplemental Material [48]) is equivalent to that found in previous works [14,38]. At small times, the propagation is ballistic and the conductivity $\sigma(\tau_i)$ increases when τ_i increases. For large τ_i, the conductivity $\sigma(\tau_i)$ decreases with increasing τ_i due to quantum interference effects and ultimately goes to zero in our case due to Anderson localization in two dimensions.

We define the microscopic conductivity σ_M as the maximum value of the conductivity over all values of τ_i. According to the renormalization theory, this value is obtained when the inelastic mean-free path $L_i(\tau_i)$ and the elastic mean-free path L_e are comparable. This microscopic conductivity σ_M represents the conductivity without the effect of quantum interferences in the diffusive regime (localization effects) and can be compared to semiclassical or self-consistent theories which also do not take into account the effect of quantum interferences in the diffusive regime.

Finally, we note that in the above formulas, it is assumed that the inelastic scattering does not affect the DOS $n(E_F)$. However, this scattering can also lead to a mixing of states that affects the DOS. In the Supplemental Material [48] (Sec. V), we analyze in detail this effect of the mixing of states. Although it is difficult to quantify, our results strongly suggest that the effect of the mixing plays a minor role except for the microscopic conductivity σ_M of the zero-energy modes where indeed the DOS varies quickly. This leads us to conclusions in contrast with those of a recent study [26] (see below and Sec. V of the Supplemental Material [48]).

Resonant adsorbates (monovacancies).—Figure 1 shows the total DOS with three different regimes consistent with previous studies [10,26]. At sufficiently large energies, the density of pure graphene is weakly affected. Near the Dirac energy, there is an intermediate regime where the pseudogap is filled. Very close to the Dirac point, there is a third regime where the density presents a peak which is reminiscent of the midgap state (also called zero-energy modes) produced by just one missing orbital.

Figure 2 shows these three regimes for the microscopic conductivity σ_M. In the first regime, i.e., at sufficiently large energies, $\sigma_M \simeq \sigma_B$, where σ_B is calculated with the Bloch-Boltzmann approach [19]. In this regime where the DOS is weakly affected (see above), $\sigma_M \gg G_0 = 2e^2/h$ and $\xi \gg L_e$ (see Secs. III and IV of the Supplemental Material [48]).

When the energy decreases, the semiclassical model fails (Fig. 2), and a second regime occurs in which $\sigma_M \simeq 4e^2/\pi h$.
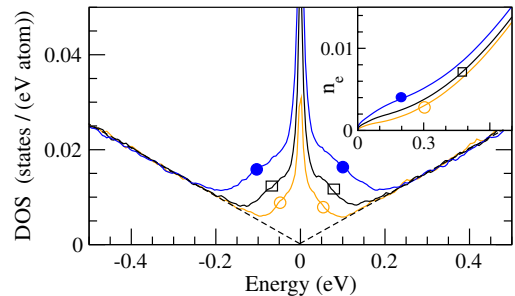
FIG. 1 (color online). Densities of states versus energy for resonant adsorbates (monovacancies) with concentrations of (empty circles) 0.1%, (empty square) 0.2%, and (filled circle) 0.4%. The dashed lines represent graphene without adsorbates. (Inset: electron density per atom n_e versus energy.)
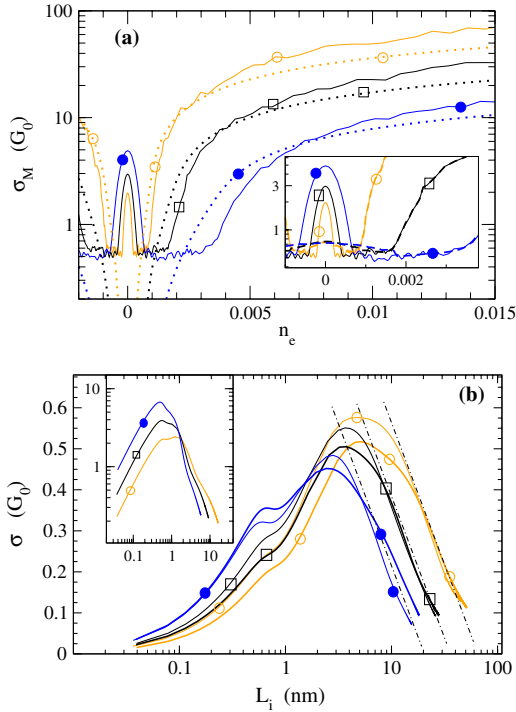
FIG. 2 (color online). Conductivity for resonant adsorbates (monovacancies) for three concentrations (see the caption of Fig. 1). (a) Microscopic conductivity σ_M versus electron density per atom n_e. The dotted lines represent predictions of the Boltzmann theory close to the Dirac energy [19]. [Inset: enlargement of the low-concentration limit: the lines represent graphene without mixing of states, the dashed lines graphene with mixing of states on an energy range $\delta E = \hbar/\tau_i$ (see Sec. V of the Supplemental Material [48]).] (b) Conductivity σ versus inelastic scattering length L_i at energies $E = 0.03$ eV (thin line) and $E = 0.04$ eV (thick line). The dot-dashed straight lines show the slope $\alpha = 0.25$ for $L_i \gg L_e$ (see the text). [Inset: $\sigma(L_i)$ at $E = 0$ in a log-log scale.] $G_0 = 2e^2/h$.

This is consistent with predictions of self-consistent theories and with numerical calculations [10,15–19,22,26]. In agreement with the literature, we find that the onset for this regime corresponds to about one electron per impurity, as shown by Fig. 2. Also, this intermediate regime occurs when the Fermi wave vector k_F is such that $k_F L_e \simeq 1$.

A characteristic length scale in this intermediate regime is the distance d between adsorbates (see the Supplemental Material [48]). Here, $d = 1/\sqrt{n}$, where n is the adsorbate density and $d \simeq 5$ nm for a concentration of 0.1%. In this intermediate regime, L_e (defined precisely in Sec. III of the Supplemental Material [48]) depends on the energy but stays comparable to d. This can be understood by noting that L_e, which according to the semiclassical theory tends to zero at the Dirac energy, cannot be much smaller than the distance d between the scattering centers.

At smaller energies, a peak of the microscopic conductivity σ_M appears very close to the Dirac energy which coincides with the peak of the DOS and represents a third regime of transport. This peak of conductivity is not predicted by self-consistent theories. It is not obtained by Refs. [18,19] and is present in the calculation of Ref. [22] although much less marked than in the present work. This peak is obtained with very similar values in the recent work [26]. In this peak, σ_M increases with the concentration of defects. Yet, σ_M is calculated here by neglecting the mixing of energy levels due to the inelastic scattering processes. As shown in the inset of Fig. 2(a), we find that this peak can decrease when the mixing of the levels due to the inelastic scattering processes is taken into account (see Sec. V of the Supplemental Material [48]).

We discuss now these three regimes for the conductivity when $L_i > L_e$ [Fig. 2(b)]. At high energies, we find standard localization effects consistent with very large localization lengths (see the Supplemental Material [48]). In the intermediate regime (i.e., $\sigma_M \simeq 4e^2/\pi h$), for concentrations 0.1% to 10%, the conductivity is well represented by the equation

$$\sigma(L_i) \simeq \frac{4e^2}{\pi h} - \alpha \frac{2e^2}{h} \log\left(\frac{L_i}{L_e}\right). \qquad (4)$$

The coefficient is $\alpha \simeq 0.25$, which is close to the result of the perturbation theory of two-dimensional Anderson localization for which $\alpha \simeq 1/\pi$ [49]. We emphasize that the regime is not perturbative close to the Dirac point. This expression shows no effect of antilocalization [50], as expected for purely short range scattering. Indeed, in that case, graphene belongs to an orthogonal symmetry class with localization effects as in a standard two-dimensional metal without spin-orbit coupling [51]. The localization length ξ deduced from this expression (4) is such that $\sigma(\xi) = 0$, which gives $\xi \simeq 13L_e$. This results justifies previous estimates of the localization length from the calculation of the elastic mean-free path that were done in this plateau of microscopic conductivity [40]. As discussed above, the elastic mean-free path L_e depends on the energy in this regime but is of the order of the distance d between adsorbates. Therefore, d determines the order of magnitude of the localization length ξ and of the elastic mean-free path L_e. More precisely, in the range of concentrations 0.1% to 10% (see Sec. IV of the Supplemental Material [48]), the localization length in this regime is $\xi \simeq 20d/r$, where the ratio r decreases with increasing energy and is $1 \leq r \leq 3$. The values of the localization length found at 10% in Ref. [24] are consistent with our study.

In the third regime where the DOS and σ_M present a peak, the conductivity does not follow the above law [Eq. (4)]. $\sigma(L_i)$ fits better with a power law $\sigma(L_i) \propto L_i^{-\beta}$, where β depends on the concentration (here, $1 < \beta < 2$). This is consistent with the divergence of the localization length ξ predicted in Ref. [23], although we do not recover the behavior found precisely at the Dirac energy. Since our energy resolution is of the order of 10^{-2} eV, we conclude that the zero-energy behavior of the conductance exists only in a narrow energy range and could be difficult to observe experimentally.
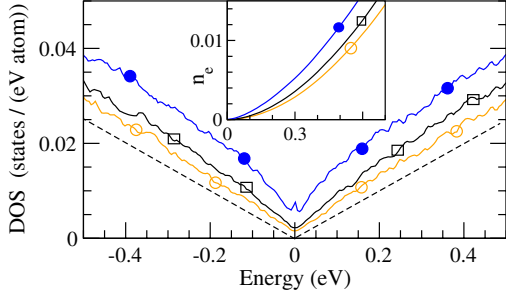
FIG. 3 (color online).　Densities of states versus energy for nonresonant adsorbates (divacancies) with concentrations 0.5% (empty circles), 1% (empty squares), and 2% (filled circle). The dashed lines represent graphene without adsorbates. (Inset: electron density per atom n_e versus energy.)

In the presence of a magnetic field, the magnetic length $L(B) = \sqrt{\hbar/eB}$ plays the role of a finite coherence length just as the inelastic mean-free path $L_i(T)$. When $L(B) < L_i(T)$, the relevant coherence length is $L(B)$ and the conductivity is $\sigma(L(B))$. This could be compared to our results, in particular, for Eq. (4).

Nonresonant adsorbates (divacancies).—Figure 3 shows the total densities of states as a function of energy for the nonresonant adsorbates. The result is similar to that obtained by the self-consistent Born approximation for Anderson disorder [15]. The two models are not strictly equivalent, but both have an energy-independent T matrix close to the Dirac energy. The microscopic conductivity σ_M presents a minimum with $\sigma_M \simeq 4e^2/\pi h$ in a narrow concentration range (Fig. 4). Again, this is consistent with the self-consistent Born approximation predictions for the Anderson model [15]. At the Dirac energy, we find that the conductivity can be represented by a power law $\sigma(L_i) \propto L_i^{-\gamma}$ with $\gamma \simeq 4$–6. Yet, Eq. (4) also fits with $\alpha \simeq 0.75$, which gives $\xi \simeq 2.5L_e$. In any case, the quick decrease of the conductivity $\sigma(L_i)$ with L_i and the narrow concentration range for the minimum of σ_M suggest that the value $\sigma_M \simeq 4e^2/\pi h$ could be very difficult to find experimentally.

A recent experimental work [52] shows that graphene with defects induced by helium ion, at about a 1% concentration, presents Anderson localization even at room temperature. Our study suggests that at such a concentration, only resonant adsorbates can create the strong localization. The length of the samples, less than 100 nm, is also consistent with small inelastic scattering [6].

Conclusion.—To conclude our study shows that the energy dependence of the scattering properties of local defects is a determinant for transport and magnetotransport properties of graphene with adsorbates. Sufficiently far from the Dirac energy, and for not too high concentrations, the semiclassical approach is usually valid. Yet, closer from the Dirac point, there are regimes where the quantum effects are essential. For resonant adsorbates, we find that
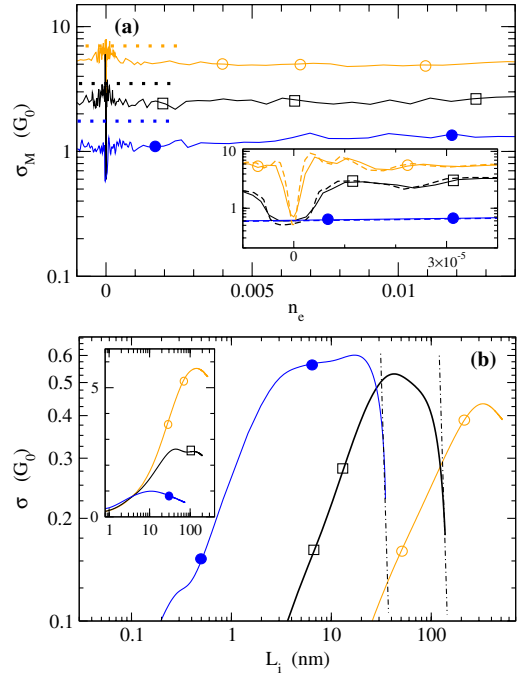
FIG. 4 (color online).　Conductivity for nonresonant adsorbates (divacancies) for three concentrations (see the caption of Fig. 3). (a) Microscopic conductivity σ_M versus electron density per atom n_e. The dotted lines represent predictions of the Boltzmann theory close to the Dirac energy. [Inset: enlargement of the low-concentration limit: the lines represent graphene without mixing of states, the dashed lines graphene with mixing of states on an energy range $\delta E = \hbar/\tau_i$ (see Sec. V of the Supplemental Material [48]).] (b) Conductivity σ versus inelastic scattering length L_i at $E = 0$ in a log-log scale. [Inset: $\sigma(L_i)$ at $E = 0.1$ eV.] $G_0 = 2e^2/h$.

in the regime of the so-called minimum conductivity, the conductivity is well represented by Eq. (4). The characteristic length scale is the distance d between defects, and the localization length ξ and the elastic mean-free path L_e are given by $\xi \simeq 13L_e \simeq 20d/r$, where the ratio r decreases with increasing energy and is $1 \lesssim r \lesssim 3$. Closer from the Dirac energy, there is a peak in the DOS which corresponds to another regime of transport in a band of midgap states. We find a critical behavior partly consistent with Refs. [23,26]. In this regime, we have shown that the inelastic scattering can destroy the peak of the DOS, which strongly affects the conductivity. Yet, a proper understanding of the physics of transport in this peak clearly requires further studies [53]. For nonresonant adsorbates, in a narrow energy range near the Dirac energy, the microscopic conductivity σ_M presents a minimum with the universal value $\sigma_M \simeq 4e^2/\pi h$. Yet, at the Dirac energy, there are strong localization effects. These could make the experimental observation of the universal value $\sigma_M \simeq 4e^2/\pi h$ very difficult. Finally, we emphasize that the methodology used here to study quantum effects for electronic transport is of wide applicability. In particular, important related

problems such as magnetoconductivity of graphene be-
yond the low field limit or competition between scattering
by defects with long range and short range potentials could
be studied as well [50].

We thank L. Magaud, C. Berger, and W. A. de Heer for
fruitful discussions and comments. The computations have
been performed at the Centre de Calcul of the Université de
Cergy-Pontoise. We thank Y. Costes and D. Domergue for
computing assistance.

---

[1] C. Berger *et al.*, J. Phys. Chem. B **108**, 19 912 (2004).
[2] K. S. Novoselov, A. K. Geim, S. V. Morozov, D. Jiang, M. I. Katsnelson, I. V. Grigorieva, S. V. Dubonos, and A. A. Firsov, Nature (London) **438**, 197 (2005).
[3] Y. Zhang, Y.-W. Tan, H. L. Stormer, and P. Kim, Nature (London) **438**, 201 (2005).
[4] C. Berger *et al.*, Science **312**, 1191 (2006).
[5] A. Hashimoto, K. Suenaga, A. Gloter, K. Urita, and S. Iijima, Nature (London) **430**, 870 (2004).
[6] X. Wu, X. Li, Z. Song, C. Berger, and W. A. de Heer, Phys. Rev. Lett. **98**, 136801 (2007).
[7] X. Wu, M. Sprinkle, X. Li, F. Ming, C. Berger, and W. de Heer, Phys. Rev. Lett. **101**, 026801 (2008).
[8] S. Y. Zhou, D. A. Siegel, A. V. Fedorov, and A. Lanzara, Phys. Rev. Lett. **101**, 086402 (2008).
[9] R. Grassi, T. Low, and M. Lundstrom, Nano Lett. **11**, 4574 (2011).
[10] N. M. R. Peres, F. Guinea, and A. H. Castro Neto, Phys. Rev. B **73**, 125411 (2006).
[11] A. Bostwick, J. McChesney, K. Emtsev, T. Seyller, K. Horn, S. Kevan, and E. Rotenberg, Phys. Rev. Lett. **103**, 056404 (2009).
[12] J. H. Chen, W. G. Cullen, C. Jang, M. S. Fuhrer, and E. D. Williams, Phys. Rev. Lett. **102**, 236805 (2009).
[13] N. Leconte, J. Moser, P. Ordejon, H. Tao, A. Lherbier, A. Bachtold, F. Alsina, C. M. Sotomayor Torres, J.-C. Charlier, and S. Roche, ACS Nano **4**, 4033 (2010).
[14] S. Roche, N. Leconte, F. Ortmann, A. Lherbier, D. Soriano, and J.-C. Charlier, Solid States Commun. **152**, 1404 (2012).
[15] T. Fukuzawa, M. Koshino, and T. Ando, J. Phys. Soc. Jpn. **78**, 094714 (2009).
[16] F. Guinea, J. Low Temp. Phys. **153**, 359 (2008).
[17] V. M. Pereira, J. M. B. Lopes dos Santos, and A. H. Castro Neto, Phys. Rev. B **77**, 115109 (2008).
[18] J. P. Robinson, H. Schomerus, L. Oroszlany, and V. I. Falko, Phys. Rev. Lett. **101**, 196803 (2008).
[19] T. O. Wehling, S. Yuan, A. I. Lichtenstein, A. K. Geim, and M. I. Katsnelson, Phys. Rev. Lett. **105**, 056802 (2010).
[20] Y. V. Skrypnyk and V. M. Loktev, Phys. Rev. B **82**, 085436 (2010).
[21] Y. V. Skrypnyk and V. M. Loktev, Phys. Rev. B **83**, 085421 (2011).
[22] A. Ferreira, J. Viana-Gomes, J. Nilsson, E. R. Mucciolo, N. M. R. Peres, and A. H. Castro Neto, Phys. Rev. B **83**, 165402 (2011).
[23] P. M. Ostrovsky, M. Titov, S. Bera, I. V. Gornyi, and A. D. Mirlin, Phys. Rev. Lett. **105**, 266803 (2010).

[24] J. Bang and K. J. Chang, Phys. Rev. B **81**, 193412 (2010).
[25] N. M. R. Peres, J. Phys. Condens. Matter **21**, 323201 (2009).
[26] A. Cresti, F. Ortmann, T. Louvet, D. Van Tuan, and S. Roche, Phys. Rev. Lett. **110**, 196601 (2013).
[27] V. M. Pereira, F. Guinea, J. M. B. Lopes dos Santos, N. M. R. Peres, and A. H. Castro Neto, Phys. Rev. Lett. **96**, 036801 (2006).
[28] A. Incze, A. Pasturel, and C. Chatillon, Surf. Sci. **537**, 55 (2003).
[29] A. Lherbier, S. M.-M. Dubois, X. Declerck, Y.-M. Niquet, S. Roche, and J.-C. Charlier, Phys. Rev. B **86**, 075402 (2012).
[30] R. R. Nair, M. Sepioni, I-L. Tsai, O. Lehtinen, J. Keinonen, A. V. Krasheninnikov, T. Thomson, A. K. Geim, and I. V. Grigorieva, Nat. Phys. **8**, 199 (2012).
[31] D. Mayou, Europhys. Lett. **6**, 549 (1988).
[32] D. Mayou and S. N. Khanna, J. Phys. I (France) **5**, 1199 (1995).
[33] S. Roche and D. Mayou, Phys. Rev. Lett. **79**, 2518 (1997).
[34] S. Roche and D. Mayou, Phys. Rev. B **60**, 322 (1999).
[35] F. Triozon, J. Vidal, R. Mosseri, and D. Mayou, Phys. Rev. B **65**, 220202 (2002).
[36] A. Lherbier, B. Biel, Y.-M. Niquet, and S. Roche, Phys. Rev. Lett. **100**, 036803 (2008).
[37] A. Lherbier, X. Blase, Y.-M. Niquet, F. Triozon, and S. Roche, Phys. Rev. Lett. **101**, 036808 (2008).
[38] G. Trambly de Laissardière and D. Mayou, Mod. Phys. Lett. B **25**, 1019 (2011).
[39] N. Leconte, A. Lherbier, F. Varchon, P. Ordejon, S. Roche, and J.-C. Charlier, Phys. Rev. B **84**, 235420 (2011).
[40] A. Lherbier, S. M.-M. Dubois, X. Declerck, S. Roche, Y.-M. Niquet, and J.-C. Charlier, Phys. Rev. Lett. **106**, 046803 (2011).
[41] N. Leconte, D. Soriano, S. Roche, P. Ordejon, J.-C. Charlier, and J. J. Palacios, ACS Nano **5**, 3987 (2011).
[42] G. Trambly de Laissardière, J.-P. Julien, and D. Mayou, Phys. Rev. Lett. **97**, 026601 (2006).
[43] C. Berger, E. Belin, and D. Mayou, Ann. Chim. (Paris) **18**, 485 (1993).
[44] E. Belin and D. Mayou, Phys. Scr. **T49A**, 356 (1993).
[45] G. Trambly de Laissardière, D. Nguyens-Manh, and D. Mayou, Prog. Mater. Sci. **50**, 679 (2005).
[46] D. Mayou, Phys. Rev. Lett. **85**, 1290 (2000).
[47] S. Ciuchi, S. Fratini, and D. Mayou, Phys. Rev. B **83**, 081202(R) (2011).
[48] See Supplemental Material at http://link.aps.org/supplemental/10.1103/PhysRevLett.111.146601 for details on the numerical method used, and additional results on the effect of inelastic scattering on conductivity and density of states.
[49] P. A. Lee and T. V. Ramakrishnan, Rev. Mod. Phys. **57**, 287 (1985).
[50] E. McCann, K. Kechedzhi, V. I. Fal'ko, H. Suzuura, T. Ando, and B. L. Altshuler, Phys. Rev. Lett. **97**, 146805 (2006).
[51] E. R. Mucciolo and C. H. Lewenkopf, J. Phys. Condens. Matter **22**, 273201 (2010).
[52] S. Nakaharai, T. Iijima, S. Ogawa, S. Suzuki, S.-L. Li, K. Tsukagoshi, S. Sato, and N. Yokoyama, ACS Nano **7**, 5694 (2013).
[53] F. Ducastelle, Phys. Rev. B **88**, 075413 (2013).